Theor Chem Account (2007) 118:495–502
DOI 10.1007/s00214-007-0364-9

REGULAR ARTICLE

Atomic many-body effects in the 4f XPS of the U^{5+} and U^{4+} cations: part II: consequences of orbital relaxation

Paul S. Bagus · Eugene S. Ilton

Received: 26 October 2006 / Accepted: 26 November 2006 / Published online: 11 July 2007

Abstract Ab initio, fully relativistic four component theory was used to determine atomic many-body effects for the 4f X-ray photoelectron spectra (XPS) of U^{5+} and U^{4+} cations. Many-body effects were included through the use of configuration interaction (CI) wavefunctions, WF's, that allow the mixing of XPS allowed and XPS forbidden configurations. This work extends our earlier study of the U 4f XPS in that the orbitals for the final, ionic states of the cations are allowed to relax in the presence of the 4f core-hole. In the earlier work, orbitals optimized for the initial state were frozen and also used for the final, ionic states. While the main XPS features are similar in both cases, using relaxed orbitals for the ionic states introduces changes in the multiplet splitting and in the $4f_{5/2}$ and $4f_{7/2}$ spin–orbit splitting. The extent of configuration mixing for the U^{5+} and U^{4+} final state WF's is characterized by the magnitude of the intensity lost by the main peaks to satellites. Overall, the use of relaxed orbitals improves the agreement between the theoretical XPS for the U^{4+} cation and the experimental measurements for UO_2.

1 Introduction

For the X-ray photoelectron spectra (XPS) of open shell systems, the ionization of a given core level normally leads to multiplet splittings of the final, ionic states of the system [1–5]. These multiplets arise from angular momentum couplings between the open core and the open valence shells. In addition to the pure angular momentum couplings, there are also many-body effects or electron correlation effects that can lead to intense satellites. These many body effects are best understood on the basis of wavefunction theory using configuration interaction (CI) wavefunctions (WF's) [2,3,5–11]. There are XPS selection rules that follow from the one-electron character of the transition operator [12–14] and that allow us to divide the configurations used in the CI WF's into XPS allowed and XPS forbidden configurations. Within the approximations used to derive the selection rules, all the XPS intensity goes into the allowed configurations where only one electron is removed from the initial state WF and no intensity at all goes into any of the other configurations, which are described as XPS forbidden. The main approximation used is that the initial state WF does not include any electron correlation effects for the core shell that is ionized; this is a reasonable approximation, especially for the calculation of the XPS intensities [5,7,9,11]. It is also common to exclude shake configurations [13] from the CI expansion for the ionic states [2,3,5–11]. However, the CI will mix XPS allowed and forbidden configurations provided that they have the same symmetry and, because of this mixing, CI final state WF's where the XPS forbidden configurations dominate may have significant intensities. We describe this as intensity stealing by the forbidden configurations from the allowed configurations and we shall examine this intensity stealing in detail for U cations.

It is common to group the angular momentum couplings, or rigorous multiplet splittings, with the many-body effects of configuration mixing and describe them both as multiplet splittings [2,3,6]. We will also describe them both as being many-body effects that cannot be described in the

Contribution to the Serafin Fraga Memorial Issue.

P. S. Bagus (✉)
University of North Texas, Department of Chemistry,
Denton, TX, USA
e-mail: bagus@unt.edu

E. S. Ilton
Pacific Northwest National Laboratory, Chemical Science Division,
Richland, WA 993, USA

framework of a single determinant WF. Many-body effects for the XPS of transition metals have been studied extensively using both semi-empirical methods, see the review in Ref. [15], where parameters are adjusted to fit experimental data and ab initio methods, see, for example, Refs. [5–8,16] where such fitting is not made. However, there have been relatively few papers providing a theoretical analysis of the XPS of actinides. Gunnarson et al. [17] and Kotani and Ogasawara [18] have studied the U 4f XPS for UO_2 and other actinide oxides but they used impurity Anderson model Hamiltonians with semi-empirical parameters and, in particular, they did not include atomic multiplet splittings. Indeed, our earlier paper on atomic many body effects in the 4f XPS of U^{5+} and U^{4+} cations [19] is the only paper we are aware of that presents ab initio relativistic results for these atomic many-body effects. Whereas inter-atomic contributions to the XPS, which include both many-body terms [20,21] and one-body terms related to the chemical bonding of the atom to its environment [8,9] are important, it is necessary to first understand the atomic effects.

In the present work, we extend our earlier analysis of many body effects on the XPS of U cations by including orbital relaxation for the final state orbitals. Specifically, we optimize the orbitals separately for the initial state where the 4f shell is filled and for the final, ionic states where the 4f shell has an electron removed. We establish that the use of either relaxed or frozen orbitals for the final state WF's gives the same general features for the U 4f XPS. We also demonstrate that the use of relaxed orbitals does lead to modest changes in the XPS, which, for U^{4+}, improve the agreement between theory and experiment [19]. We discuss the reasons that the use of relaxed orbitals lead to changes in the relative energies $E_{\rm rel}$, and the relative intensities, $I_{\rm rel}$, of the XPS peaks and we explain why these changes go in different directions for U^{5+} and U^{4+}. We also examine the extent to which XPS forbidden configurations steal intensity from the XPS allowed configurations. The loss of intensity to satellites dominated by forbidden configurations provides a useful measure of the importance of many-body effects due to configuration mixing.

The organization of the paper is as follows. Section 2 discusses the methods for the calculation of the relativistic WF's and for the calculation of the intensities of the XPS peaks. This is followed in Sect. 3 by a discussion of the theoretical XPS spectra for the U cations, which focuses on a comparison of the results using relaxed orbitals with the earlier results obtained with frozen orbitals; for the U^{4+} XPS, a comparison is also made to the experimental XPS for UO_2 [19]. A detailed analysis of the changes in the U^{5+} XPS spectra is given in Sect. 3.2 and the analysis of the U^{4+} XPS spectra is given in Sect. 3.3. Finally, our conclusions are summarized in Sect. 4.

2 Theoretical methods

The results reported here, as well as in our previous paper, [19] referred to as Part I, are based on relativistic Dirac–Fock self-consistent field, DF–SCF, and Dirac CI, DCI, calculations. The theoretical formalisms for the DF–SCF and DCI calculations are described in Ref. [22]. The calculations in Part I were performed using the MOLFDIR program system [22] while the new calculations reported in this paper were performed using the DIRAC program system, [23] which offers greater flexibility for performing open shell DF–SCF calculations. The initial open shell occupations for U^{5+} and U^{4+} are $5f^1$ and $5f^2$, respectively while the open shell configurations for the 4f ionized states are $4f^{13}5f^1$ and $4f^{13}5f^2$, respectively. The DF–SCF calculations are carried out for the average of configurations for the ground and 4f ionized configurations of the two U cations. The average of configurations includes the distribution of the electrons in the open shells in all ways over the $f_{5/2}$ and $f_{7/2}$ spin–orbit split sub-shells. With MOLFDIR [22], we were able only to perform DF–SCF calculations for the ground state configurations; with DIRAC [23], we are able to optimize 4-component spinors for both the ground state and the 4f-hole configurations. The spinors optimized for the ground state configurations for the cations are then used to determine DCI WF's for the different states and levels arising from this configuration. The spinors optimized for the 4f-hole configurations are used for the DCI WF's for the final, 4f ionized, states and levels. There is no question that the relaxed orbitals will give much better absolute energies for the final state WF's [24]. However, a key issue that is answered by the present work is the extent to which the choice of relaxed or frozen spinors will affect the $E_{\rm rel}$ of the different ionic levels.

In both Part I and the present work, the same extended basis set of Gaussian type orbitals (GTO's) were used; the exponents for these GTO's were optimized [25] for calculations on UO_2^{2+}. However, in the present work, the GTO's were not contracted while, in Part I, the GTO's that describe the core spinors, especially the deep cores, were very heavily contracted in order to reduce the size of the Fock matrices that have to be diagonalized. Because a non-segmented contraction scheme [25] was used, we do not expect the contraction to significantly change relative energies. As a test, we examined the spin–orbit splittings of the 4f DF–SCF orbital energies for the ground state configurations. Between the MOLFDIR and DIRAC calculations for both U^{5+} and U^{4+}, the spin–orbit splittings changed by less than 0.0003 eV; these changes are sufficiently small to insure that the contraction used in Part I would not account for the differences between those and the present calculations. Other parameters for the DF–SCF and DCI calculations, in particular for the

finite nuclear size and the integral classes retained, are the same as used in Part I.

The DCI WF's are designed to include near degeneracy effects important for the XPS [2,3,5,6,9,11] within and between the open 4f and 5f shells. For the ground state of $U^{4+}(5f^2)$, the CI includes determinants where the two 5f electrons are distributed in all possible ways over the 14 5f spinors. This CI gives a balanced treatment of j–j and L–S coupling within the 5f shell and properly represents intermediate coupling [26,27]. It leads to a ground state $J = 4$ level that is, as expected from the 5f spin–orbit splitting of ∼1 eV, dominated by the $5f^2_{5/2}$ configuration. The first excited level is $J = 5$ at $\Delta E = 0.73$ eV. For the ground state of U^{5+}, the H-matrix over the determinants with the one 5f electron in all spinors is diagonal. The lowest level is $J = 5/2$ and the $J = 7/2$ level is at $\Delta E = 0.93$ eV. For the 4f-hole states, the DCI introduces new many-body electron correlation effects. As for the ground states, the one or two 5f electrons are distributed in all possible ways over the 14 5f spinors but now all 14 positions of the 4f hole are combined with these distributions of the 5f electrons. The new effect introduced is the angular momentum coupling and recoupling within and between the 4f and 5f shells. These many-body effects were introduced to treat the p-shell XPS of transition metal TM, cations [2,3,11] and are standardly included for the TM p-shell XPS [5,6,8,9,21,28,29]. We have extended the logic of this treatment and applied it to ab initio studies of the 4f XPS of U [19]. However, especially for heavy atoms, additional near degeneracy effects may become important; see, for example, studies of alkaline earth atoms by Kim and Bagus [30]. For actinides, these additional near degeneracy effects could involve redistribution of electrons within the 6s, 6p, 6d, and 7s sub-shells. Despite the potential importance of these other terms, our treatment of the angular momentum coupling and recoupling for the 4f and 5f electrons is a zeroth order step to including atomic many body effects for actinides.

In preparation for the analysis of the 4f XPS peaks for U cations [19], it is useful to consider the 4f XPS allowed J levels. We will distinguish between the peaks due to pure multiplet split levels and the satellites due to the configuration mixing of these XPS allowed configurations with the XPS forbidden configurations. The XPS allowed configurations for 4f ionization of U^{5+} are $4f^6_{5/2}4f^7_{7/2}5f^1_{5/2}$ and $4f^5_{5/2}4f^8_{7/2}5f^1_{5/2}$; these configurations couple to $J = 1, 2, 3, 4, 5, 6$ and to $J = 0, 1, 2, 3, 4, 5$, respectively [26]. For the 4f ionization of U^{4+}, the allowed configurations all have the $5f^2_{5/2}$ shell coupled to a $J = 4$ level that then couples with the open $4f^7_{7/2}$ or $4f^5_{5/2}$ shells to couple to $J = 1/2$ through $J = 15/2$ levels or to $J = 3/2$ through $J = 13/2$ levels [26]. As shown in Sect. 3, the configuration mixing of the allowed and forbidden configurations affects not only the XPS I_{rel} but also the E_{rel} of the dominantly XPS allowed 4f-hole levels.

In order to determine the I_{rel} of the XPS peaks, we use the sudden approximation [13] SA, suitably extended for open shell initial states [4,14]. The SA assumes that at the instant of photoionization, the ionized state is described by a WF where a core electron has been annihilated from the ground state wavefunction. The I_{rel} for a particular ionic level or multiplet is then proportional to the sum over the many electron overlaps for the WF's for that level with the annihilated ground state WF. Suitable summation over ionization of different spinors and averages over degenerate initial states must also be made [4,12,31]. When different, mutually non-orthogonal, orbitals sets are used for the initial and for the final, ionic WF's, the calculation of the many-electron overlap integrals is significantly more complicated than when a single orbital set is used [32]. To determine the SA I_{rel}, we have calculated the many electron overlap integrals exactly using a cofactor formalism [33,34]. The program for these calculations is based on code for the calculation of matrix elements between non-relativistic WF's [35] that we have extended to handle relativistic WFs built from four-component spinors.

3 U 4f XPS spectra: results and discussion

3.1 General considerations

In Figs. 1 and 2, we give the theoretical 4f XPS spectra for U^{4+} and U^{5+}, respectively; in the upper panel of each figure, we give the results obtained in the present work using relaxed orbitals for the final states while in the lower panel, we show the results from Part I obtained using frozen, ground state orbitals for the ionic, 4f-hole states. The calculated peaks for individual ionic levels, or for sets of ionic levels that are very closely spaced in energy, are represented by Gaussians broadened to 0.9 eV full width at half maximum (FWHM). This broadening is introduced to take account of the finite energy width of the X-ray photons, of the lifetime of the U 4f-holes, and of instrumental resolution [6,19]. The sums of the individual peaks are shown and this envelope represents the full calculated XPS spectra. For the U^{4+} XPS in Fig. 1, we include a comparison with the experimental XPS for $UO_{2.15}$, Ref. [19], which is dominantly U^{4+}. The positions of the theoretical curves for the U^{4+} cation were rigidly shifted to give the best agreement with the first, $4f_{7/2}$, peak of the experimental XPS. This is the only adjustment to the calculated values. The E_{rel} and I_{rel} calculated for the various final, ionic states are exactly as obtained from our ab initio calculations. For the U^{5+} XPS in Fig. 2, the position of the theoretical curves were placed on the same energy scale as

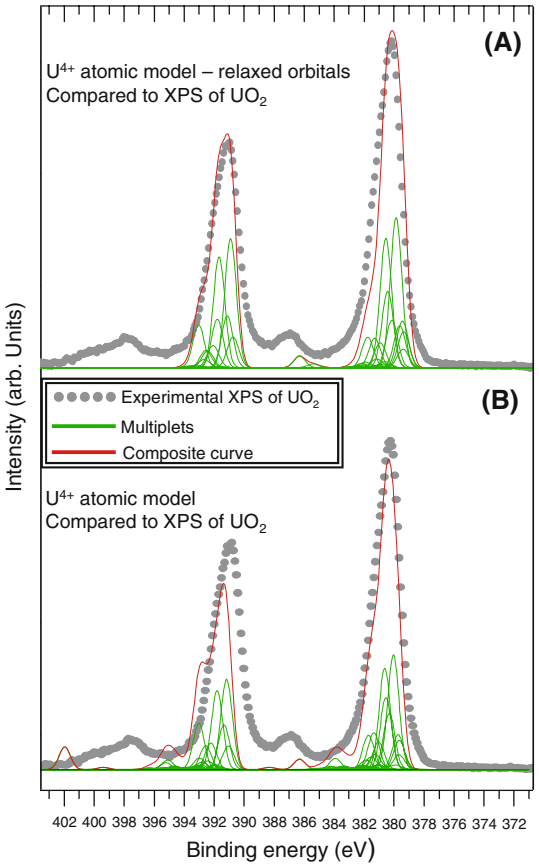

Fig. 1 Theoretical U(4f) XPS for the free U^{4+} ion using the relaxed orbitals for the final, ionic states, upper curves (**a**), and using frozen orbitals, lower curves (**b**). The energies of the theoretical curves are shifted rigidly to give the best fit to the experimental XPS, also shown. The theoretical I_{rel} are broadened with a Gaussian function, see text. The contributions of individual 4f-hole final states are shown in *green* while the sum of these individual contributions is the composite curve in *red*

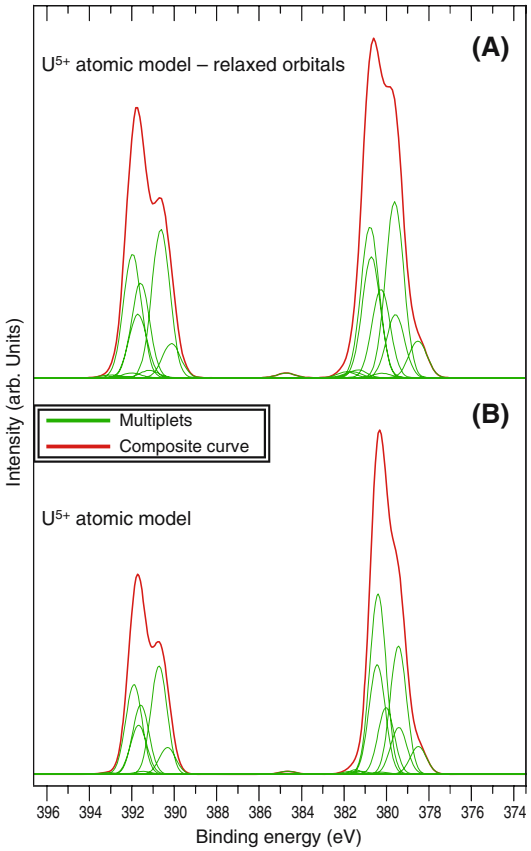

Fig. 2 Theoretical U(4f) XPS for the free U^{5+} ion using the relaxed orbitals for the final, ionic states, upper curves (**a**), and using frozen orbitals, lower curves (**b**). The absolute energy scale is not related to experiment, see text. For other features of the XPS curves, see the caption to Fig. 1

for U^{4+}, but the absolute energies of the multiplets are not related to experiment.

The main features of the theoretical curves with the relaxed and frozen orbitals for the 4f-hole states are reasonably similar. Both the theoretical and experimental XPS spectra have only two dominant peaks arising from $4f_{7/2}$ and $4f_{5/2}$ ionization and separated by a spin–orbit splitting of ∼11 eV. While these peaks are ∼ 2 eV FWHM broad, they are composed of contributions from many individual multiplet split levels. The U^{4+} 4f XPS, Fig. 1, is considered first. Here, the most important difference between the two theoretical spectra is that the spin–orbit splitting of the $4f_{7/2}$ and $4f_{5/2}$ peaks is reduced by ∼ 0.5 eV when relaxed orbitals are used for the final, ionic states, Fig. 1a. With the relaxed orbitals, this splitting is in significantly closer agreement with experiment. In addition, the intensities of low-lying satellites are significantly reduced when relaxed orbitals are used. For the $4f_{7/2}$ peak, the satellites at ∼384 eV are essentially missing and for the $4f_{5/2}$ peak, the satellites at ∼ 395 eV are missing from the relaxed orbital spectra. Also, the intensity of the satellites at ∼ 393 eV are significantly lower so that the shoulder in the frozen orbital $4f_{5/2}$ XPS peak, Fig. 1b, is absent from the relaxed orbital peak; this change brings the shape of the $4f_{5/2}$ peak into better agreement with experiment. We also note that the $4f_{7/2}$ peak is slightly narrower when the relaxed orbitals are used. As we will discuss in detail below, this is the opposite of the change in FWHM that we would expect when the more contracted relaxed 5f orbitals are used. We will show that all of these differences can be related to a smaller configuration mixing between XPS allowed and XPS forbidden configurations when relaxed orbitals, instead of frozen orbitals, are used. Finally, we note that the ∼ 6 eV satellites of both the $4f_{7/2}$ and $4f_{5/2}$ peaks are not well represented in either the frozen or the relaxed orbital XPS spectra. These peaks have been assigned to inter-atomic charge transfer satellites [17–19,36] and, hence, we do not expect them to be present in our model, which does not include condensed phase effects. Turning to the U^{5+} XPS, the most noticeable difference between the relaxed and frozen orbital spectra is

a broadening of the $4f_{7/2}$ and $4f_{5/2}$ peaks by ~ 0.5 eV when the relaxed orbitals are used. Since this change has a simpler origin, we consider first the U^{5+} 4f XPS and then we discuss the more complex case of the U^{4+} XPS where cancelling contributions contribute to the differences between the frozen and the relaxed orbital spectra.

3.2 Analysis of the U^{5+} XPS

In Table 1, we give the E_{rel} and the SA I_{rel} for the levels that are dominated by the XPS allowed configurations, either $4f^6_{5/2}4f^7_{7/2}5f^1_{5/2}$, also denoted $4f^{-1}_{7/2}5f^1_{5/2}$, or $4f^5_{5/2}4f^8_{7/2}5f^1_{5/2}$, also denoted $4f^{-1}_{5/2}5f^1_{5/2}$. The different multiplet split levels are denoted by their J value; possible J values were discussed in Sect. 2. Results are given for the use of frozen orbitals in the final state DCI and for the use of relaxed orbitals with spinors optimized for the 4f-hole configuration. The E_{rel} are given with respect to $E_{rel} = 0$ for the lowest energy, $J = 1$, level for $4f_{7/2}$ ionization; for the $4f_{5/2}$ multiplets, the energy spacings of the different levels are given as ΔE_{rel} with $\Delta E_{rel} = 0$ for the lowest energy level, $J = 1$, within this group. The normalization of the I_{rel} has been chosen to directly indicate the intensity that is lost from states dominated by the XPS allowed configurations. The SA intensity that goes to an XPS allowed configuration coupled to a particular J value is proportional to the multiplicity; i.e., to $2J+1$ [4,12,14]. When relaxed orbitals are used for the final state WF's, these intensity ratios will be modified if there is differential relaxation of the spin–orbit split spinors for $j = \ell+1/2$ and $j = \ell - 1/2$. In the present cases, this differential relaxation is negligible and changes the $2J+1$ intensity factor by ≤ 0.001. The directly computed I_{rel} for our DCI WF's are all multiplied by a constant factor that would give $I_{rel} = 2J+1$, for allowed, or $I_{rel} = 0$, for forbidden configurations, if there were no configuration mixing between the XPS allowed and forbidden configurations. Thus the amounts by which these normalized I_{rel} are less than $2J+1$, denoted in Table 1 as Lost I and given as a percent reduction, are direct measures of the intensity lost to XPS satellites through configuration mixing.

The intensity lost to satellites is not especially large. For the $4f_{7/2}$ final states, the intensities lost from the main XPS peaks for the different J levels range between 0 and 11% and are similar for the frozen and relaxed orbital calculations but slightly larger using the relaxed orbitals. These small losses indicate that the XPS peaks are dominated by allowed configurations. For the $4f_{7/2}$ peaks, the energies for the different J levels range over ~ 2 eV for both frozen and relaxed orbital calculations. However, the energy separations are larger, by $\sim$ 0.2–0.3 eV, when relaxed orbitals, rather than frozen orbitals, are used. We ascribe this difference to changes in the 4f,5f exchange integrals [9,37] when the 5f orbital relaxes in response to the presence of the 4f-hole. Since the 5f orbital sees a larger effective nuclear charge when there is a 4f-hole, the 5f orbital will be contracted relative to the orbital for the initial state of U with a filled 4f shell. This orbital contraction leads, in turn, to larger values of the exchange integrals. Since the diagonal energies of the different J level couplings of the configurations depend on the magnitudes of the 4f,5f exchange integrals [26,37], we expect larger energy spacings when relaxed orbitals are used. The contraction of the 5f spinors will also lead to an increase of the DCI off-diagonal matrix elements because they also depend on these exchange and closely related integrals [37]. In turn, this can be responsible for the increase in the configuration mixing, which leads to a slightly greater loss of intensity into satellites when relaxed orbitals are used.

The general behavior of the $4f_{5/2}$ multiplet split peaks follows that for the $4f_{7/2}$ multiplets. Little intensity is lost to satellites; the greatest losses are for the $J = 1$ and the $J = 0$ levels that carry the lowest XPS intensities. The intensity lost to the satellites is somewhat larger when relaxed orbitals are used. Except for the $J = 0$ level, discussed in more detail

Table 1 For the main $4f^{-1}_{7/2}$ and $4f^{-1}_{5/2}$ XPS peaks for 4f-hole levels of U^{5+}, E_{rel} and ΔE_{rel}, in eV, and SA I_{rel}, normalized as described in the text, are given for the relaxed and frozen orbital 4f-hole WF's for each of the allowed J values

J[a]	Relaxed orbial WF's		Frozen orbital WF's	
	$E_{rel}/\Delta E_{rel}$	I_{rel}/lost I (%)	$E_{rel}/\Delta E_{rel}$	I_{rel}/lost I (%)
$4f^{-1}_{7/2}$				
1	0	2.67/11.1	0	2.78/7.4
2	1.08	4.58/8.3	0.93	4.70/6.0
6	1.11	12.80/1.5	0.94	12.85/1.2
3	1.75	6.44/8.0	1.52	6.68/4.5
4	2.22	8.79/2.3	1.91	8.87/1.4
5	2.26	10.99/0.1	1.96	10.99/0.1
$4f^{-1}_{5/2}$				
1	11.63/0	2.48/17.4	11.83/0	2.70/10.0
5	12.13/0.50	10.80/1.9	12.24/0.40	10.84/1.4
3	13.09/1.46	6.88/1.8	13.08/1.25	6.94/0.9
2	13.21/1.58	4.64/7.2	13.18/1.35	4.91/1.8
4	13.48/1.85	8.99/0.0	13.42/1.58	9.00/0.0
0	28.38/16.75	0.66/34.2	26.13/14.30	0.69/31.0

The intensity lost to XPS satellites, for each J value, is given in the column labeled Lost I as a percent of the total I_{rel} going into an allowed 4f-hole configuration with this J value

[a] Note the energetic order of the different J couplings does not follow either a monotonically increasing or decreasing order as usually expected, see Ref. [26]; the configuration mixing of XPS forbidden with the XPS allowed configurations may be responsible for the irregular order of the energies for the J values

below, the separation of the multiplet split peaks, as given by E_{rel} and ΔE_{rel}, is $\sim$ 1.6–$\sim$ 1.9 eV with the larger value for the relaxed orbitals. For the peaks that carry the largest intensities $J = 2$–$J = 5$, the values of E_{rel} are quite similar between the relaxed and frozen orbital calculations. The relaxed orbital value of E_{rel} for $J = 5$ is 0.1 eV smaller, the value for $J = 4$ is 0.1 eV larger and the values for $J = 2$ and 3 are essentially the same between the relaxed and frozen orbital calculations. This is consistent with essentially the same apparent $4f_{7/2}$ to $4f_{5/2}$ spin–orbit splitting of the XPS peaks with relaxed and frozen orbitals.

With relaxed orbitals, the main $J = 0$ XPS peak is at $E_{rel} = 28.4$ eV with 66% of the XPS intensity for $J = 0$ peaks; similar values are found with frozen orbitals. We discuss this peak, which is very far from the peaks for the remainder of the levels associated with $4f_{5/2}$ ionization, in order to demonstrate that CI may shift the excited states to higher energies, in contrast to the case of ground states, where CI always lowers the energy. In our DCI, there are two configurations that couple to $J = 0$ arising from $\Phi_1 = 4f^{-1}_{5/2}5f^{1}_{5/2}$ and $\Phi_2 = 4f^{-1}_{7/2}5f^{1}_{7/2}$ where Φ_1 is XPS allowed and Φ_2 is XPS forbidden. From the DF–SCF orbital energies, the 5f spin–orbit splitting is $\sim$ 1 eV while the 4f spin–orbit splitting is $\sim$ 11 eV. Thus, the diagonal energy of the XPS forbidden configuration Φ_2, is lower by $\sim$ 10 eV than the diagonal energy of Φ_1 since Φ_1 involves removing a more tightly bound $4f_{5/2}$ electron. The two $J = 0$ roots of the DCI are a lowest root at $E_{rel} = 6.2$ eV with 34% of the $J = 0$ intensity and the higher, dominantly XPS allowed, root at $E_{rel} = 28.4$ eV. For a 2×2 CI, the lowest root is shifted by an energy Δ below the lowest diagonal energy while the upper root is shifted by an equal amount Δ, above the higher diagonal energy [38]. The fact that shifts in the energies due to CI may be to larger energies for excited states is relevant for the change of the apparent spin–orbit splitting in the XPS of the U^{4+} cation, discussed below.

3.3 Analysis of the U^{4+} XPS

In Table 2, we give the E_{rel} and the I_{rel} for the levels that, for a given J value carry the largest I_{rel}; these values are compared for the relaxed and frozen orbital WF's for the 4f ionized final states of $U^{4+}(5f^2_{5/2};\ J = 4)$. With one exception, these states are dominated by XPS allowed configurations, as for the U^{5+} XPS. The exception is the $4f^{-1}_{5/2}$ $J = 5/2$ level where the intensity is distributed over several levels, see below. The definitions for E_{rel}, ΔE_{rel}, and the normalization of I_{rel} to the multiplicity of the final, ionic levels is the same as used in Table 1; as in Table 1, the quantity Lost I is also given. Extremely important differences of the U^{4+} final states from those for U^{5+} are related to the extent of configuration mixing as displayed by the quantities Lost I. For U^{5+}, the XPS was mainly to levels that were strongly dominated by the XPS allowed configurations; see Table 1. For the relaxed orbital results, there are only three levels that lose more than 10% of the intensity going into the XPS allowed configurations.

Table 2 For the main $4f^{-1}_{7/2}$ and $4f^{-1}_{5/2}$ XPS peaks for 4f-hole levels of U^{4+}, E_{rel} and ΔE_{rel}, in eV, and SA I_{rel} are given for the relaxed and frozen orbital 4f-hole WF's for each of the allowed J values; see the caption for Table 1 for definitions of the quantities given

J[a]	Relaxed orbial WF's		Frozen orbital WF's	
	$E_{rel}/\Delta E_{rel}$	I_{rel}/lost I (%)	$E_{rel}/\Delta E_{rel}$	I_{rel}/lost I (%)
$4f^{-1}_{7/2}$				
3/2	0	3.80/4.9	0	3.05/23.7
1/2	0.05	1.96/2.0	0.03	1.53/23.5
5/2	0.09	4.91/18.1	0.09	3.63/40.0
7/2	0.27	4.42/44.8	0.25	4.72/41.1
15/2	0.51	15.80/1.2	0.41	11.98/25.1
9/2	0.79	5.02/49.8	0.70	5.83/41.7
11/2	1.08	8.05/32.9	0.92	7.52/37.4
13/2	1.18	13.63/2.7	0.99	10.54/24.7
$4f^{-1}_{5/2}$				
3/2	11.31/0	3.22/19.4	11.50/0	2.46/38.6
13/2	11.46/0.15	13.64/2.6	11.66/0.11	9.41/32.8
7/2	11.68/0.37	5.45/31.9	11.86/0.30	4.65/41.8
11/2	12.24/0.92	11.70/2.5	12.31/0.76	8.24/31.4
9/2	12.35/1.03	5.12/48.8	12.44/0.89	5.08/49.2
5/2	12.63/1.32	2.34/61.0	12.74/1.18	2.74/45.6

[a] See footnote to Table 1

The situation is quite different for the 4f XPS of U^{4+}. For the frozen orbital results for the $J = 5/2$, 7/2, and 9/2 levels for both $4f^{-1}_{7/2}$ and $4f^{-1}_{5/2}$, over 40% of the I_{rel} is lost to satellites and the lowest loss to satellites is 23.5% for the $J = 1/2$ level for $4f^{-1}_{7/2}$. These losses are recovered in satellites, especially around $\Delta E_{rel} \approx$ 3–4 eV; see Fig. 1. For the relaxed orbital WF's, there is generally much less loss of intensity from the most intense peaks of a given J value. In particular, for the $J = 15/2$ level of $4f^{-1}_{7/2}$, only 1.2% of the intensity is lost to satellites compared to 25% when frozen orbitals are used and for $J = 13/2$ only $\sim$2.5% of I_{rel} is lost to satellites for both $4f^{-1}_{7/2}$ and $4f^{-1}_{7/2}$; these losses should be compared to the losses of more than 25% for the same levels when frozen orbitals are used. We speculate that the greater configuration mixing for the frozen orbital WF's arises because different $5f^2$ distributions, over the $5f_{7/2}$ and $5f_{5/2}$ spinors, may help overcome the limitations of the frozen 5f orbitals when there is a 4f-hole. In effect, the greater importance of configuration mixing when frozen 5f orbitals are used is likely to be an artifact due to using the unrelaxed 5f spinors; one that will

lead to greater I_{rel} for the satellites. There are cases with the relaxed orbitals where there are large losses from the main peaks; in particular, for the $4f^{-1}_{7/2}$ $J = 7/2$ and 9/2 and for the $4f^{-1}_{5/2}$ $J = 9/2$ and 5/2 and this does lead to some intensity in the satellites. Overall, the reduction in the intensity losses to satellites, when relaxed orbitals are used, leads to an effective narrowing of the peaks, which is, especially for the $4f_{5/2}$ peak, in better agreement with the XPS for UO_2. As for the U^{5+} XPS, discussed above, using the relaxed orbitals leads to small increases in the spread of energies of the main peaks, of ~0.1–0.2 eV, and we ascribe these increases to the contraction of the 5f orbital due to the 4f-hole. However here, the increases of the peak widths due to these small increases in energy spacing are more than offset by the decrease in intensity in the satellites.

The main relaxed orbital $4f^{-1}_{5/2}$ peaks for $J = 3/2$–$J = 9/2$, which are in the energy range E_{rel} = 11.3–12.6 eV are all at smaller E_{rel} than found with the frozen orbitals by ~0.1–0.2 eV. This lowering of E_{rel}, combined with the fact that all these main peaks carry greater intensity when the relaxed orbitals are used, leads to an apparent reduction in the $4f^{-1}_{7/2}$–$4f^{-1}_{5/2}$ spin–orbit splitting and to an improvement in the agreement with the XPS experiment for UO_2. In our discussion of the $J = 0$ main and satellite peaks of the U^{5+} XPS, we pointed out that the CI energies for excited states could lead to increases in E_{rel}. Since, the CI mixings are smaller for the DCI with relaxed orbitals for these excited levels, this could contribute to somewhat lower E_{rel}. In effect, the reduction of the CI artifacts due to using 5f spinors that are optimized for the presence of the 4f-hole not only reduces the satellite intensities but it also improves the 4f spin–orbit splitting compared to measured XPS values for UO_2.

The relaxed orbital $4f^{-1}_{5/2}$ $J = 5/2$ peak at $E_{rel} = 12.6$ eV receives only 39% of the $4f^{-1}_{5/2}$ intensity going into $J = 5/2$ final states. Most of the remaining intensity goes to satellites at $E_{rel} = 6.9$ eV with 20% of the intensity and at 25.6 eV with 36% of the intensity. The 25.6 eV satellite is just past the energy cut-off for the curves in Fig. 1a. However, when frozen orbitals are used, there is a high energy $J = 5/2$ peak at $E_{rel} = 23.4$ eV with 26% of the $J = 5/2$ intensity; this peak is just inside the energy cut-off and can be seen in Fig. 1b. This high energy peak does not appear to be present in the UO_2 XPS. It is possible that the peak is an artifact because we have used a limited orbital space for the DCI that, in the valence space, was restricted to the 5f spinors. By analogy with the higher lying, nearly degenerate orbitals included in the active spaces for CI calculations of transition metal cations [7], it is possible that other orbitals should be included in the active space for the U cation DCI. Such orbitals could include the 6p and 6d. An extended active space CI involving additional atomic many-electron effects might yield additional satellite intensity.

4 Concluding remarks

We have examined the contributions of atomic many-body effects to the U 4f XPS for U^{4+} and U^{5+} free ions. The many body-effects were treated within the theoretical formalism of configuration mixing and represent the angular momentum coupling and recoupling within and between the core level, 4f, and valence level, 5f, open shells. This treatment of atomic many body effects has been extensively used for the XPS of transition metal cations and we have applied it here for actinide cations. The present work represents an extension of our prior work in that we have allowed the orbitals to relax in the presence of a 4f-hole in the ionic states. The variational re-optimization of the final, ionic state orbitals leads to contracted orbitals that provide an improved representation of the outer, valence shells.

While the overall features of the predicted XPS spectra are similar for the relaxed and frozen orbital calculations, there are differences in the details of the widths of the XPS peaks and the apparent 4f spin–orbit splitting. We have related these differences to two aspects of the relaxed orbital wavefunctions. The relaxed orbitals for the outer shells are contracted when a core-hole is present relative to the orbitals for the initial state configuration. This leads to an increase in the separation of the multiplet energies and to an increase in the FWHM of the $4f_{5/2}$ and $4f_{7/2}$ XPS peaks for U^{5+}. However, in the case of U^{4+} where there is a $5f^2$ occupation, the use of relaxed orbitals reduces the extent of the configuration mixing and, thus, reduces the intensity of the XPS satellites. For the frozen orbital case, the larger configuration mixing has been described as an artifact due to the use of frozen orbitals for the outer 5f, shell. Important consequences of the reduction of configuration mixing are reduced FWHM of the 4f XPS peaks for U^{4+} and reduced apparent spin–orbit splitting of the $4f_{5/2}$ and $4f_{7/2}$ XPS peaks; both of these changes improve the agreement of the U^{4+} theoretical predictions with XPS measurements for UO_2.

Acknowledgments This research was supported by the Geosciences Research Program, Office of Basic Energy Sciences, U. S. Department of Energy. P.S.B. is pleased to acknowledge partial computer support from the National Center for Supercomputing Applications, Urbana-Champaign, IN. We would also like to thank Dr. W. A. DeJong for helpful discussions. Material in this paper was included in an invited presentation at an ACTINET meeting sponsored by SCK-CEN, on 22 June, 2006 at Mol, Belgium.

References

1. Fadley CS, Shirley DA, Freeman AJ, Bagus PS, Mallow JV (1969) Phys Rev Lett 23:1397
2. Gupta RP, Sen SK (1974) Phys Rev B 10:71
3. Gupta RP, Sen SK (1975) Phys Rev B 12:15

4. Bagus PS, Schrenk M, Davis DW, Shirley DA (1974) Phys Rev A 9:1090
5. Bagus PS, Broer R, de Jong WA, Nieuwpoort WC, Parmigiani F, Sangaletti L (2000) Phys Rev Lett 84:2259
6. Ilton ES, deJong WA, Bagus PS (2003) Phys Rev B 68:125106
7. Bagus PS, Broer R, Ilton ES (2004) Chem Phys Lett 394:150
8. Bagus PS, Ilton ES, Rustad JR (2004) Phys Rev B 69:205112
9. Bagus PS, Ilton ES (2006) Phys Rev B 73:155110
10. Bagus PS, Viinikka EK (1977) Phys Rev A 15:1486
11. Freeman AJ, Bagus PS, Mallow JV (1973) Int J Magn 4:35
12. Bethe HA, Salpeter EW (1957) Quantum mechanics of one- and two-electron atoms. Academic, New York
13. Åberg T (1967) Phys Rev 156:35
14. Sangaletti L, Parmigiani F, Bagus PS (2002) Phys Rev B 66: 115106
15. de Groot FMF (1994) J Electron Spectrosc Relat Phenom 67:529
16. Bagus PS, Woll C, Ilton ES (2006) Chem Phys Lett 428:207
17. Gunnarsson O, Sarma DD, Hillebrecht FU, Schonhammer K (1988) J Appl Phys 63:3676
18. Kotani A, Ogasawara H (1993) Physica B 16: 186–188
19. Ilton ES, Bagus PS (2005) Phys Rev B 71:195121
20. Zaanen J, Westra C, Sawatzky GA (1986) Phys Rev B 33:8060
21. Okada K, Kotani A (1992) J Phys Soc Jpn 61:4619
22. Visscher L, Visser O, Aerts PJC, Merenga H, Nieuwpoort WC (1994) Comput Phys Commun 81:120
23. Saue T, Bakken V, Enevoldsen T, Helgaker T, Jensen HJA, Laerdahl JK, Ruud K, Thyssen J, Visscher L (2000) Dirac, a relativistic ab initio electronic structure program, Release 3.2.
24. Bagus PS, Illas F, Pacchioni G, Parmigiani F (1999) J Electron Spectrosc Relat Phenom 100:215
25. de Jong WA, Visscher L, Nieuwpoort WC (1999) Theochem 458:41
26. Condon EU, Shortly GH (1951) The theory of atomic spectra. Cambridge University Press, Cambridge
27. Briancon C, Desclaux JP (1976) Phys Rev A 13:2157
28. Taguchi M, Uozumi T, Kotani A (1997) J Phys Soc Jpn 66:247
29. Taguchi M, Uozumi T, Okada K, Ogasawara H, Kotani A (2001) Phys Rev Lett 86:3692
30. Kim YK, Bagus PS (1973) Phys Rev A 8:1739
31. Sangaletti L, Depero LE, Bagus PS, Parmigiani F (1995) Chem Phys Lett 245:463
32. Löwdin PO (1955) Phys Rev 97:1474
33. Prosser F, Hagstrom S (1968) Int J Quantum Chem 2:89
34. Prosser F, Hagstrom S (1968) J Chem Phys 48:4807
35. McLean AD, Yoshimine M, Lengsfield BH, Bagus PS, Liu B (1990) In: Clementi E Modern techniques in computational chemistry. MOTECC-90. ESCOM Science Publishers B.V, Leidon, p 593
36. Ilton ES, Boily J-F, Bagus PS (2007) Surf Sci 601:908
37. Slater JC (1960) Quantum theory of atomic structure, vols I and II. McGraw-Hill, New York
38. Schiff LI (1968) Quantum mechanics. McGraw-Hill, New York